JOURNAL OF MATERIALS SCIENCE 26 (1991) 112–116

Formation of metastable t′-phase in solute-redistributed Y-PSZ

S. J. LIN, H. Y. LU, P. SHEN
Institute of Materials Science and Engineering, National Sun Yat-Sen University, Kaohsiung, Taiwan

Owing to solute redistribution by a liquid phase analogue of diffusion-induced grain-boundary migration metastable and anti-phase domain boundary-bearing tetragonal (t′) phase was seen to occur in the cubic (c) matrix grain of sintered (1400 °C, 2 h) and furnace-cooled yttria-partially stabilized zirconia (Y-PSZ) specimens (TZ3Y + 12Y-PSZ in molar ratios of 4:1, 1:1 and 1:4). In contrast to that formed by rapid cooling, t′-phase formed by slow cooling shows no deformation accommodation twins. Subsequent ageing at 1100 °C for up to 240 h caused the formation of finely tweed (c) and tetragonal (t) assemblages at the expense of coarse tweed t′-phase in the 12Y-PSZ grains. The absence of secondary deformation twins in the t′-phase formed by slow cooling is discussed.

1. Introduction

High solute and anti-phase domain boundary (APB)-bearing tetragonal phase, which does not transform martensitically to the monoclinic phase, has been observed in yttria-partially stabilized zirconia (Y-PSZ) and designated t′-phase, to differentiate it from the equilibrium t-precipitate in the cubic (c) matrix [1–3]. In addition to the primary t′-twin variants, secondary fine {1 0 1} deformation twins have been recognized in fine-grained polycrystals [4] and in plasma-sprayed materials [5]. It is generally believed that t′-phase forms by rapid cooling from the c-phase of suitable solute content (locus between C_0* and the univariant line of t/c + t) ([4] and literature cited therein) and the transformation was a displacive, thermal dissipation-related type [4]. The c–t′ transformation was also found in the c-matrix of a two-phase alloy of Y-PSZ [6, 7]. The slowly cooled single-crystal two-phase alloy (8 wt % Y_2O_3) heated at 1600 °C for 50 h also shows APB-like features in the matrix which are similar to those of t′-phase, although tweed c + t array is also a likely interpretation [6]. Chemical inhomogeneity commonly occurs in sintered PSZ due to the solute redistribution on approaching equilibrium [8], or due to the dissolution of other alloying elements, e.g. Ni_2AlTi [9, 10] and NiAl [9]. The c-phase of a solute content suitable for the formation of t′-phase may possibly occur in these sintered Y-PSZ and affect the transformation toughening effect. Here the formation of t′-phase in a solute redistributed c-matrix of the original Y-PSZ powder (12 wt % Y_2O_3) sintered at 1400 °C with TZ3Y (3 mol % Y_2O_3) additives and slowly cooled, is reported. The subsequent microstructure development on ageing at 1100 °C was also studied.

2. Experimental procedure

Powder mixtures of TZ3Y (3 mol % Y_2O_3, Toyo Soda, Tokyo, Japan) and 12Y-PSZ (12 wt % Y_2O_3, Zircar Products Inc., USA) in molar ratios of 4:1, 1:1 and 1:4, were die-pressed (100 MPa), sintered at 1400 °C for 2 h and cooled to room temperature (~ 15 min from 1400 to 1200 °C, then about 4 h to 25 °C) in an open furnace. The sintered discs were subjected to ageing at 1100 °C for 94, 120 and 240 h and cooled in the same furnace. Scanning electron microscopy (SEM, Jeol, JSM35CF instrument at 25 kV) coupled with energy dispersive X-ray (EDX) analysis was used to analyse the grain size and qualitative composition. The fired discs were analysed by X-ray diffraction (Cu$K\alpha$, 35 kV, 25 mA) for phase identification. Step scanning was also carried out with a diffractometer using Cu$K\alpha$ radiation (35 kV, 25 mA, step size 0.03°, fixed counts 30 sec) over two ranges of 2θ values covering the {1 1 1} and {4 0 0} diffraction peaks of zirconia, the zirconia phases being indexed as a slightly distorted version of the c-fluorite unit cell. The {4 0 0} peaks were deconvoluted assuming individual gaussian peaks for the zirconia phases. The integrated peak areas were then converted to molar fractions of zirconia phases using the formulae given by Miller *et al.* [3]. Thin sections prepared from sintered discs were ion-milled and studied by transmission electron microscopy (TEM, Jeol-200CX instrument operating at 200 kV).

---

*C_0 designates the intersection point of the free energy curves (temperature against composition) of c- and t-ZrO_2 phase.

0022–2461/91 $03.00 + .12

3. Results

3.1. As-sintered (1400 °C, 2 h)

Regardless of the amount of TZ3Y added, the as-sintered samples contained larger 12Y-PSZ and t-zirconia (TZ3Y) grains (Fig. 1) which is similar to the bimodal grain-size distribution in the sintered TZ3Y with added MgO [11]. Zirconia phases of t, c and m symmetry were identified by X-ray diffraction from the as-fired discs. Because grinding causes an appreciable change in the content of m-phase, some t-phase was considered to be transformable rather than nontransformable t′-phase. TEM observation, however, indicates the presence of t′-phase (Fig. 2a) with characteristic APBs when some 12Y-PSZ grains were imaged with the $\{1\,1\,2\}$ diffraction spot. Most of the

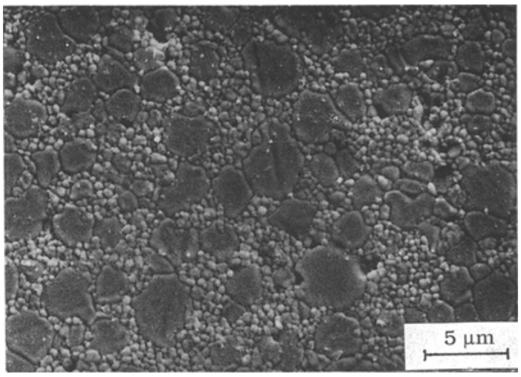

Figure 1 Secondary electron image of as-sintered (1400 °C, 2 h) and slowly cooled specimen (TZ3Y : 12Y-PSZ = 1 : 4).

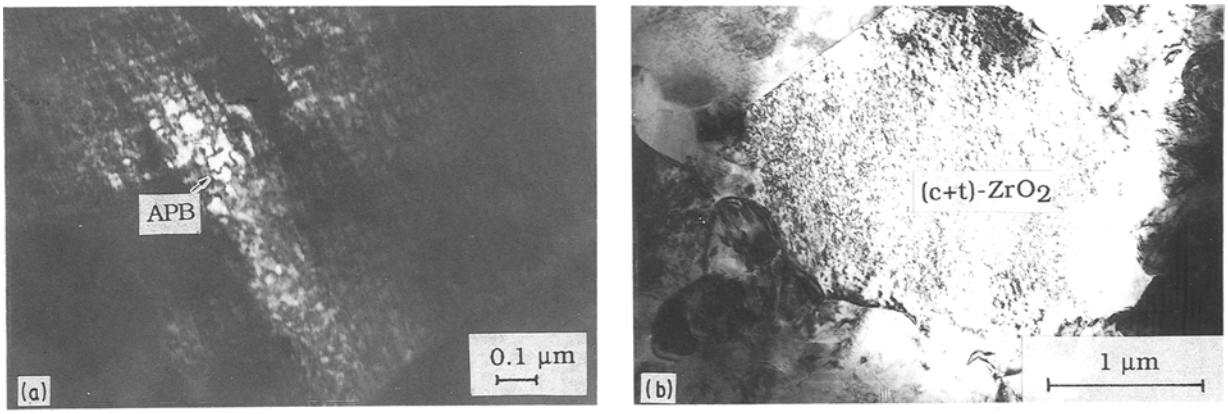

Figure 2 Transmission electron micrograph of large 12Y-PSZ grains: (a) dark-field image ($g = \{1\,1\,2\}$) of t′-variant showing APBs, (b) bright-field image of tweed c + t, same specimen as Fig. 1.

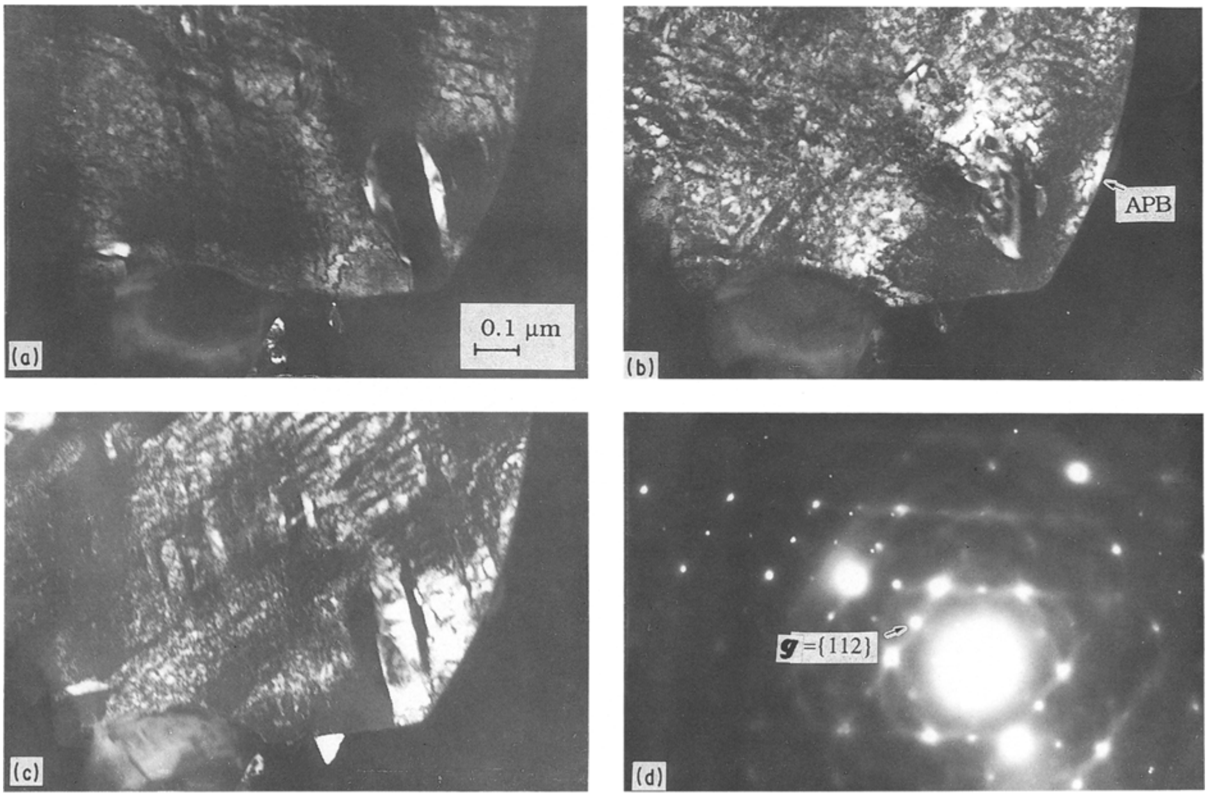

Figure 3 Dark-field image ($g = \{2\,1\,1\}$) of nearly 100% t + t′-grain showing APB (arrow) in variants of primary twin (a to c), (d) SAD pattern ($Z = [1\,1\,1]$), same specimen as Fig. 1.

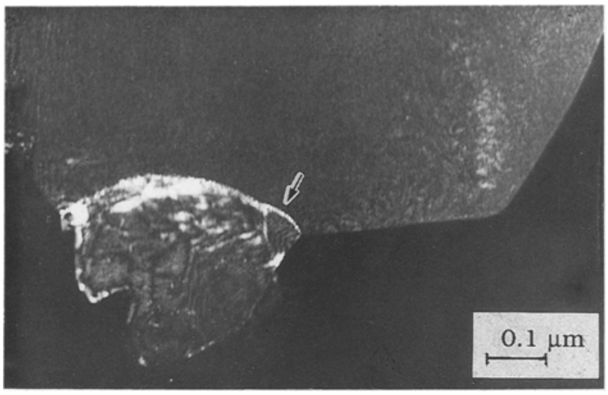

Figure 4 Dark-field image ($\boldsymbol{g} = \{1\,1\,2\}$) of misfit dislocation (arrow) at semicoherent interface of coalesced tweed grain and t-grain, same specimen as Fig. 1.

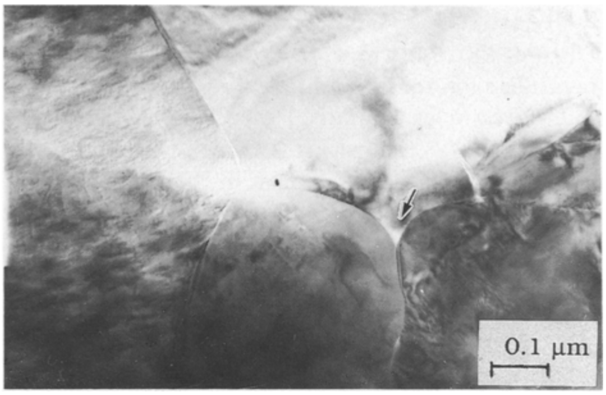

Figure 5 Bright-field image showing glassy phase (arrow) of the same specimen as Fig. 1.

12Y-PSZ grains show tweed contrast (Fig. 2b) due to the precipitation of t-precipitates in the c-matrix. Occasionally, domain-bearing t′ variants filling nearly the whole 12Y-PSZ grain were observed (Fig. 3) indicating c–t′ transformation has occurred in the c-matrix. Note that the t′-phase has characteristic APB in contrast to the APB-free t-grain. The [1 1 1] SAD patterns were used to distinguish t′-phase from c-phase [6], and are also useful to distinguish t′-phase from o- and m-phases which may have APB-like features in Y-PSZ, (Mg, Y)-PSZ and possibly in Mg-PSZ systems [12]. The semicoherent boundary between tweed grains and t-grains indicates coalescence has occurred (Fig. 4). A glassy phase at the grain boundary and grain corners indicates the occurrence of eutectic melting (Fig. 5).

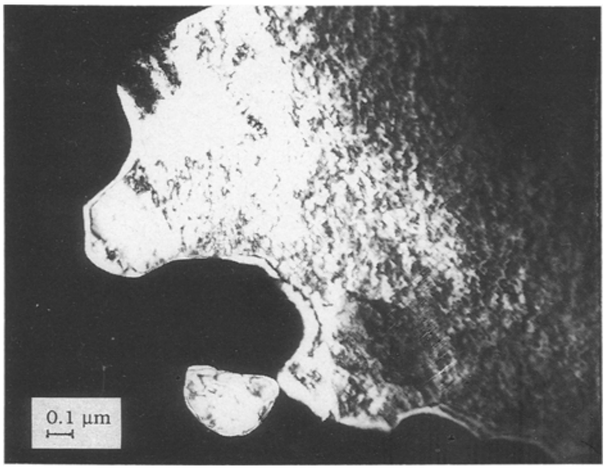

Figure 6 Dark-field image ($\boldsymbol{g} = \{0\,2\,0\}$) showing corrugated grain boundary of a tweed grain, aged at 1100 °C for 120 h and slowly cooled (TZ3Y : 12Y-PSZ = 1 : 4).

3.2. Postsintering ageing (1100 °C for 94, 120 and 240 h)

The corrugated grain boundary of the tweed grain (Fig. 6) and the incorporation of t-zirconia grains within the tweed grain forming a semicoherent interface were commonly observed in aged specimens regardless of ageing time and the amount of TZ3Y added (Fig. 7). Some APB in the tweed grain survived the early ageing treatment; however, the variant width and domain size were significantly smaller than those of the as-sintered specimens. Upon ageing, t′-phase decomposed into lower solute-bearing t-phase and higher solute-bearing c-phase; however, the decomposition reaction was not complete for 120 h ageing at 1100 °C. Tweed grains similar to that of as-sintered specimens were still observed for ageing up to 240 h; however, inhomogeneity was indicated by the patches showing coarse and fine tweed (about 20 to 30 nm in

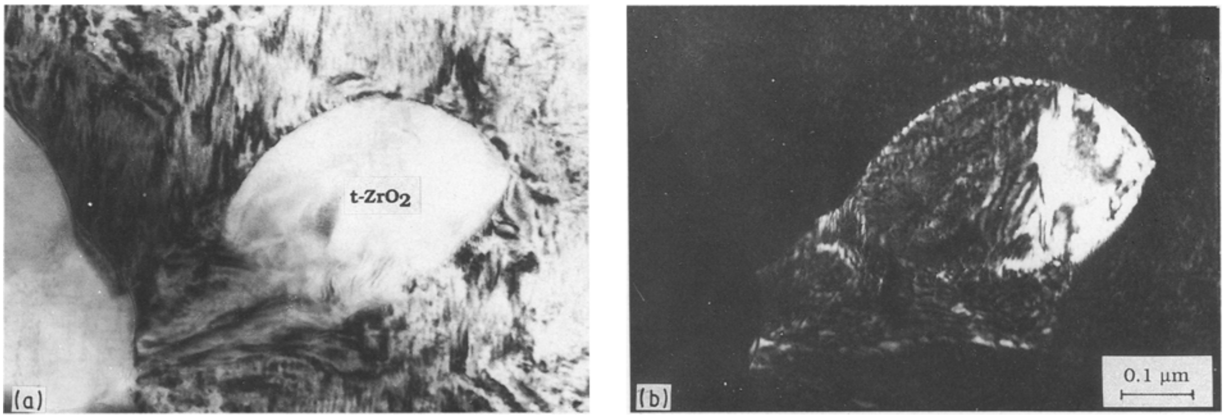

Figure 7 Transmission electron micrograph showing incorporation of a t-grain into a tweed grain: (a) bright-field image, (b) dark-field image ($\boldsymbol{g} = \{2\,1\,1\}$), same specimen as Fig. 6.

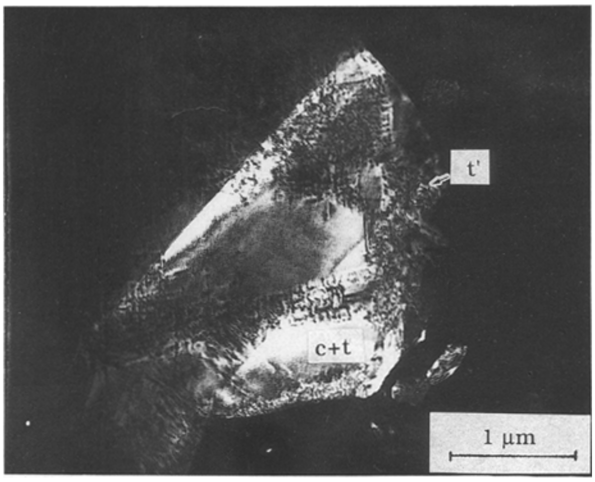

Figure 8 Dark-field image ($g = \{2\,1\,1\}$) of tweed grain showing coarse tweed t'-phase and fine tweed c + t array in a specimen aged at 1100 °C for 240 h and slowly cooled (TZ3Y : 12Y-PSZ = 4 : 1).

size) regions (Fig. 8) which probably represent the retained t'-phase and the newly formed c + t phase assemblages, respectively. Growth of these (c + t + t') grains by the capillarity effect was indicated by the curvature of the grain boundary (Fig. 9). Some m-grains were found in aged specimens, indicating t–m transformation has probably occurred in TZ3Y grain during cooling from 1100 °C (Fig. 10).

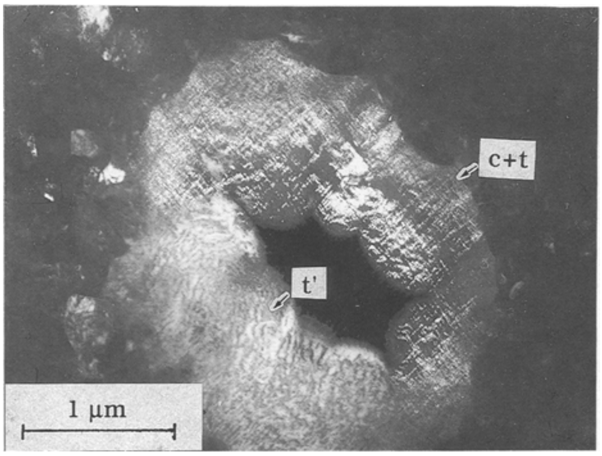

Figure 9 Dark-field image ($g = \{1\,1\,2\}$) showing coarsened c + t + t' grain in the same specimen as Fig. 8.

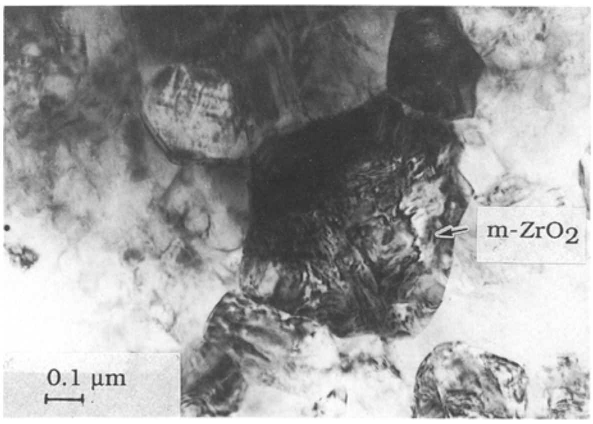

Figure 10 Bright-field image of m-grain in the same specimen as Fig. 8.

3.3. EDX analysis

SEM-EDX analysis of the as-sintered specimens indicates the tweed grain has a significantly higher count ratio of Y/Zr than for the t-grain, and a composition variation was detected near the grain boundary. The t-precipitates and the incorporated t-grain, caused interference with SEM-EDX and STEM-EDX analyses on the fine or coarse tweed array of aged specimens; however, a higher count ratio of Y/Zr is still obtained for tweed grain than for t-grain.

4. Discussion

4.1. Solute redistribution by sintering

The domain size (50 to 60 nm) within each t' plate of as-sintered specimens seems independent of zirconia grain size, and the domain size of 50 nm corresponds to C_0 of 5 mol % Y_2O_3 according to the relationship of domain size and yttria content in Y-PSZ [13]. This indicates the 12Y-PSZ (6.9 mol % Y_2O_3) grain has been modified to a lower solute content during sintering. It is likely that the solute content of the c-matrix in the original Y-PSZ powder was lowered during sintering at 1400 °C due to its mixture with solute-poor TZ3Y, so that transformation to t'-phase by cooling through T_0 (about 1100 to 1200 °C, see locus of C_0–temperature in Figs 1 and 2 of [4]) was allowed. Because slow cooling retains t'-phase, the t'–c + t transformation requires an incubation time as shown by ageing the plasma-sprayed Y-PSZ [5]. The semicoherent interface containing misfit dislocations between the tweed grain and the t-grain suggests that the solute redistribution proceeds by diffusion-induced grain-boundary migration (DIGM) [14] in addition to the capillarity effect. The glassy phase at grain boundary and triple junctions or grain corners further suggests that a liquid-phase analogue of DIGM [15] may also occur.

4.2. Decomposition of t'-phase by ageing

Postsintering ageing at 1100 °C caused the decomposition of t'-phase into equilibrium c + t phase assemblages regardless of the amount of TZ3Y added; however, the decomposition was not complete for up to 120 h because domain-like features were retained in the coarse tweed region. The fine tweed region of 120 h sample and almost the whole tweed grain of the 240 h aged specimen have a tweed array similar to that observed by Lanteri *et al.* [6]. The fine tweed array is approximately 20 to 30 nm in aged specimens. The locus of C_0 at 1100 °C is about 8.5 wt % (4.8 mol %) Y_2O_3 [4]. According to the relationship between domain size and solute content [13], the anti-phase domain size is larger than 50 nm if the c-phase of the Y_2O_3 content of less than 8.5 wt % transforms into the t'-phase at T_0 lower than the ageing temperature of 1100 °C. It follows that the t'-phase is a relic rather than a decomposition product t'-phase newly formed from a non-equilibrium and ZrO_2-rich (between C_0 and t/c + t univariant at a temperature slightly lower than 1100 °C) c-phase. It is likely that the newly formed c-phase at 1100 °C has a solute content within the locus of C_0 and the c/c + t univariant line of Heuer *et al.* [4], hence no c–t′ transformation occurred during cooling.

4.3. Characteristics of t′-phase formed by slow cooling

The tweed array in the present aged specimens is similar to that of the two-phase alloy single-crystal Y-PSZ (8 wt % Y_2O_3) heated (1600 °C, 50 h) and slowly cooled [6]. The tweed arrays thus formed were interpreted either as t′-phase or equilibrium c + t phase assemblages [6]. The slowly cooled Y-PSZ specimens sintered at 1400 °C, however, show unambiguous evidence of t′-phase (Fig. 2a). The t′-phase formed by slow cooling has slightly different morphology compared to the quenched phase [4, 5, 13]. The t′-ZrO_2 is always characterized by twin variants containing APBs which arise because of the lowering of symmetry during transformation ([4] and literature cited therein). In addition to the primary t′-twin variants, secondary fine $\{1\,0\,1\}$ deformation twins were recognized in fine-grained polycrystals [4] and in plasma-sprayed materials [5] but only rarely in skull-melted single crystals. These secondary t′ twins were attributed to deformation due to the tetragonality of t′-phase. No such fine twins were observed in the present samples indicating quenching was probably required to induce martensitic-like transformation so that deformation accommodation twins (secondary) can form. It is less likely that the formation of the secondary t′-twins depends on C_0, because martensitic features were observed in arc-melted Y-PSZ of various compositions (3 to 5 mol % Y_2O_3) [13]. A two-step development of t′-phase in arc-melted ZrO_2–Y_2O_3 alloys has been suggested: APBs are formed initially and plate-like or lenticular features form later [13]. It is likely that only the first step occurred during slow cooling of the present sintered or aged Y-PSZ specimens so that only APB features were formed.

5. Conclusions

1. Metastable t′-phase was formed in solute-redistributed Y-PSZ (12Y-PSZ with TZ3Y addition in molar ratios of 4:1, 1:1 and 1:4) after sintering at 1400 °C and slowly cooling.

2. Anti-phase domain boundaries (APB) but no deformation twins were found in the t′-phase of the slowly cooled specimen.

3. Subsequent ageing at 1100 °C for up to 240 h caused the formation of fine tweed c- and t-phase assemblages at the expense of coarse tweed t′-phase in the 12Y-PSZ grain.

Acknowledgements

This research was supported in part by ITRI and the National Science Council of Taiwan.

References

1. J. LEFEVRE, *Ann. Chim.* **8** (1963) 118 (in French).
2. H. G. SCOTT, *J. Mater. Sci.* **10** (1975) 1527.
3. R. A. MILLER, J. C. SMIALEK and R. G. GARLICK, in "Science and Technology of Zirconia, Advances in Ceramics", Vol. 3, edited by A. H. Heuer and L. W. Hobbs (The American Ceramic Society, Columbus, Ohio, 1981) p. 241.
4. A. H. HEUER, R. CHAIM and V. LANTERI, *Acta Metall.* **35** (1987) 661.
5. S. CHEN and P. SHEN, *Mater. Sci. Engng A.*, **114** (1989) 159.
6. V. LANTERI, R. CHAIM and A. H. HEUER, *J. Am. Ceram. Soc.* **69** (1986) C-258.
7. N. ISHIZAWA, A. SAIKI, T. YAGI and N. MIZUTANI, *ibid.* **69** (1986) C-262.
8. B. V. N. RAO and T. P. SCHREIBER, *ibid.* **65** (1982) C-44.
9. P. SHEN and S. L. HWANG, *Mater. Sci. Engng* **100** (1988) 177.
10. P. T. CHAO and P. SHEN, *ibid.* **A 117** (1989) 191.
11. H. Y. LU and J. S. BOW, *J. Amer. Ceram. Soc.* **72** (1989) 228.
12. A. H. HEUER, V. LANTERI, S. C. FARMER, R. CHAIM, R. R. LEE, B. W. KIBBEL and R. M. DICKERSON, *J. Mater. Sci.* **24** (1989) 124.
13. T. SAKUMA, *ibid.* **22** (1987) 4470.
14. R. W. BALLUFFI and J. W. CAHN, *Acta Metall.* **29** (1981) 493 and literature cited therein.
15. E. P. BUTLER and A. H. HEUER, *J. Amer. Ceram. Soc.* **68** (1985) 197.

Received 8 August 1989
and accepted 19 February 1990